PRAMANA
— journal of
physics

Vol. 71, No. 6
December 2008
pp. 1353–1366

Effect of solar features and interplanetary parameters on geomagnetosphere during solar cycle-23

SANTOSH KUMAR* and AMITA RAIZADA
Department of P.G. Studies and Research in Physics and Electronics, R.D. University, Jabalpur 482 001, India
*Corresponding author. E-mail: s_kumar123@rediffmail.com

MS received 14 January 2008; revised 13 June 2008; accepted 24 June 2008

Abstract. The dependence of geomagnetic activity on solar features and interplanetary (IP) parameters is investigated. Sixty-seven intense (-200 nT $\leq$ Dst < -100 nT) and seventeen superintense (Dst < -200 nT) geomagnetic storms (GMSs) have been studied from January 1996 to April 2006. The number of intense and superintense GMSs show three distinct peaks during the 11-year period of 23rd solar cycle. The largest number of high strength GMSs are observed during maximum phase of solar cycle. Halo and partial halo CMEs are likely to be the major cause for these GMSs of high intensity. No relationship is observed between storm duration and the number of CMEs involved in its occurrence. The intensity of the GMS is also independent of the number of CMEs causing the occurrence of storm. These geoeffective CMEs show western and northern bias. Majority of the geoeffective CMEs are associated with X-ray solar flares (SFs). Solar and IP parameters, e.g., $V_{\rm CME}$, $V_{\rm SW}$, B, B_z (GSE and GSM coordinates) and their products, e.g., $V_{\rm SW}{\cdot}B$ and $V_{\rm SW}{\cdot}B_z$ are observed and correlated to predict the occurrence of intense GMSs. $V_{\rm CME}$ does not seem to be the appropriate parameter with the correlation coefficient, $r = -0.2$ with Dst index, whereas the correlation coefficient, $r = -0.57$, -0.65, 0.75, -0.68 and 0.77 of the parameters $V_{\rm SW}$, B, B_z, $V_{\rm SW} \cdot B$ and $V_{\rm SW} \cdot B_z$ respectively, with Dst indicating that $V_{\rm SW} \cdot B_z$ and B_z may be treated as the significant contributors in determining the strength of GMSs.

Keywords. Coronal mass ejections; solar flares; solar wind; interplanetary magnetic field; magnetic reconnection; geomagnetic storms.

PACS Nos 96.60.ph; 96.60.qe; 96.50.Ci; 96.50.Bh

1. Introduction

The likely causes of GMSs have been investigated by various research groups [1–3], so as to predict their occurrence and intensity well in advance. The geospheric environment is highly affected by the Sun and its features such as solar flares (SFs), active prominences and disappearing filaments (APDFs), coronal holes, coronal mass ejections (CMEs), etc. Research in the past three decades identifies CMEs as

the most energetic events in the heliosphere. CMEs are now understood as large-scale magnetized plasma structures originating from closed magnetic field regions the Sun: active regions, filament regions, active region complexes and transequatorial interconnecting regions [4].

CMEs from the Sun drive solar wind (SW) disturbances in terms of magnetic field, speed and density, which in turn cause magnetic disturbance in Earth [2]. It has been established by now that GMSs occur when the southward component of interplanetary magnetic field (IMF), B_z, impinges upon the Earth's magnetosphere and reconnects [5]. The main cause of intense GMSs is believed to be the large IMF structure which has an intense and long duration southward magnetic field component, B_z [6,7]. They interact with the Earth's magetic field and facilitate the transport of energy into the Earth's atmosphere through the reconnection process. Earth-directed CMEs are likely to impact the magnetosphere to cause GMS [4,8]. The intensity of GMS is primarily decided by the speed of CME and strength of magnetic field it contains [4,9], whereas according to Manoharan [8], primary factors determining the geoeffectiveness are the direction of propagation of CMEs, its speed, size, density, orientation and strength of the magnetic field at the near Earth space. Intense GMSs are found to be mainly caused by CMEs [2,5,10,11].

CMEs are associated with a number of phenomena like radiobursts, flares, prominence eruptions (PEs), solar energetic particles (SEPs) etc. The simple connection between solar eruptions and their geospace consequences gets complicated when CMEs interact. CMEs may collide with one another resulting in the change of trajectories or merger. The GMSs may become quite extended and complex when CMEs are ejected in quick succession [5]. The frequency of CMEs varies with sunspot cycle. At solar minimum, there is about one CME/week. Near solar maximum, 2 to 3 CMEs/day on an average are observed. CMEs are often associated with SFs and PEs. Somehow, they may also occur in the absence of either of these processes [12].

The purpose of this paper is to identify the solar features with their detailed characteristics and IP parameters which are likely to cause intense and superintense GMSs. In the present paper, the intense and superintense GMSs have been investigated from January 1996 to April 2006 based on disturbance storm time (Dst) index. As given by Loewe and Prolss [13], GMSs may be classified into five groups based on the minimum value of Dst: weak (-30 nT $>$ Dst ≥ -50 nT), moderate (-50 nT $>$ Dst ≥ -100 nT), strong (-100 nT $>$ Dst ≥ -200 nT), severe (-200 nT $>$ Dst ≥ -350 nT) and great (Dst < -350 nT). Somehow, we have used the term intense for strong GMSs and superintense for severe and great GMSs which is similar to Gonzalez *et al* [14] and Srivastava and Venkatakrishnan [3]. Thus, the intense GMSs will be designated with -100 nT $>$ Dst ≥ -200 nT; whereas superintense GMSs with Dst < -200 nT.

The solar characteristics of the identified geoeffective CMEs, which are responsible these GMSs have been studied. CMEs with an apparent width of 360° are taken as 'halo', whereas the CMEs with width $\geq$120° and $\leq$359° are taken as 'partial halo' [11,15]. CMEs are known to reach Earth in the time scale of 1 to 5 days which roughly depend on the initial speed of CMEs [2]. Occasionally, CMEs take less than a day to reach Earth [11]. The travel time of CME from its appearance at the solar disk to the time of commencement of GMS and the time when GMS is

at its peak are analysed and correlated. How the intensity of GMS is related to the average value of IMF (B) and B_z in GSE and GSM coordinates are investigated. Further, solar surface distribution of geoeffective CMEs and their association with SFs and APDFs is observed.

2. Data and its analysis

During the period of January 1996 to April 2006, 90 GMSs which are of intense and superintense nature, i.e. Dst < -100 nT have been selected, out of which 84 GMSs have been investigated leaving six GMSs due to data gaps in SOHO/LASCO CME catalogue. The values of Dst indices are taken from World Data Center, Japan (http://swdcwww.kugi.kyoto-u.ac.jp). Solar geophysical data and SOHO/LASCO CME Catalogue are used to study storm sudden commencement (SSC) and manifestations of CMEs causing intense GMSs as well as association of SFs and APDFs with these CMEs. Location of halo CMEs responsible for causing intense GMSs have been cross-verified by the data available at http://cdaw.gsfc.nasa.gov/publications/gopal2007.halo_dst.table.pdf. A criterion similar to Kumar and Yadav [16] is followed to determine the solar source of GMSs. On the basis of solar wind velocity (V_{SW}), solar features have been identified. OMNIWEB data are used to obtain the values of SW while ACE data helped in providing the IMF values.

3. Results and discussion

3.1 *Variation of solar activity*

The solar activity is analysed on the basis of sunspot numbers (SSNs) present over the solar disk during solar cycle-23. The largest value of the sunspot acquired in a year has been plotted yearly in figure 1. Solar cycle-23 rises slowly in the beginning,

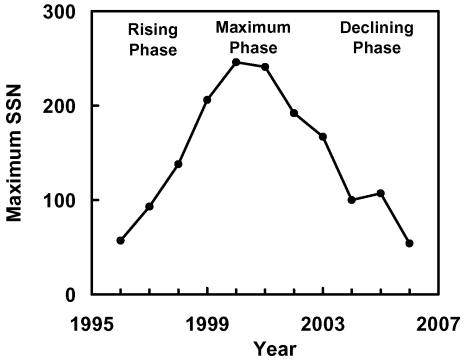

Figure 1. Yearly variation of solar activity with maximum sunspot number of the year.

depicting a smooth maxima between 1999 and 2002 acquiring the maximum value of sunspots, i.e., 246 in the year 2000 which is the largest in the 23rd cycle and then declines up to 2004 with SSN becoming 100. It again takes a pick up in 2005 with SSN becoming 107 and then falls to 54 in 2006. The SSNs observed during the start and end phases of solar cycle are almost same (i.e. 57 and 54 in 1996 and 2006 respectively). Thus, it is implied that solar cycle-23 started from minimum activity of SSNs in 1996, attaining maximum value in 2000 and falling back to almost the same activity of SSNs in 2006. The entire period under consideration, as shown in figure 1, is divided into three parts: Rising phase from 1996 to 1998, maximum phase from 1999 to 2002 and declining phase from 2003 to 2006, which is almost the same duration as used by Gopalswamy *et al* [11]. However, extended period from 1996 to 2006 has been used in the present investigation.

3.2 *Geomagnetic storms*

Out of the 90 GMSs observed during the years 1996 to 2006, 80% are of intense and 20% are of superintense nature. Highly variable conditions in the Sun and in the geospace environment persist throughout the maximum phase of solar activity [17]. Since the number of CMEs varies with the solar cycle, intense geomagnetic activity triggered by CMEs is expected to be more important at solar maximum [10]. Thus, one expects a large number of GMSs with Dst < -100 nT close to the solar maximum, which is also observed in the present study and is depicted in figure 2. Almost similar observation is made by Zhang *et al* [18], who have observed that the yearly major storm rate is highest during 2000–2002, around the time of maximum SSN, whereas the occurrence rate is lowest in 1996 at solar minimum. The number of GMSs of intense and superintense nature during maximum phase, i.e. in the years 2000, 2001 and 2002 are 14, 14 and 13 respectively, which is significantly high as compared to rising and declining phases. However, there is a significant decline in the number of GMSs in the year 1999 as compared to 1998. The year 1999 is termed as 'conspicuous' by Srivastava and Venkatakrishnan [3] and 'anomalous' by Cid *et al* [10] and Gopalswamy *et al* [11]. Low number of magnetic clouds are observed in 1999 [19,20], which may be responsible for causing lesser number of GMSs. Like SSNs, yearly variation of the number of intense and superintense GMSs also show three part structure which is clear from figure 2. During both the years of minimum activity i.e., 1996 and 2006, the number of intense GMSs is just one with almost similar Dst values, i.e. -105 nT and -111 nT respectively. Hence, the largest number of high strength GMSs are observed during maximum phase of solar cycle.

3.3 *Geomagnetic indices*

It is observed that the Dst index starts decreasing much before the onset of GMSs, attaining its minimum value when storm is at its peak and starts increasing again till it reaches almost the same initial value. Thus, there is a time delay between the onset of GMS and the time when Dst reaches its minimum value. The variation in

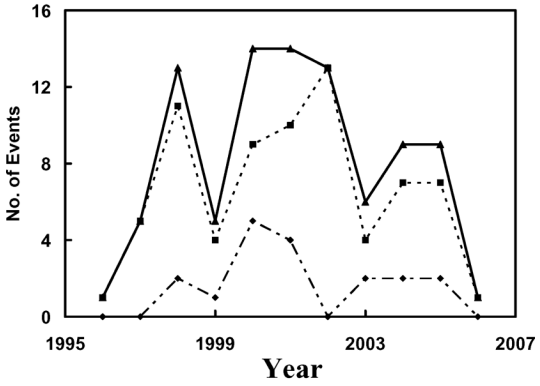

Figure 2. Yearly variation of intense (■), superintense (♦) and total (▲) GMSs during solar cycle-23.

delay time is from a minimum of 4 h to a maximum of 56 h in the present study. This time delay is understandable because the occurrence of a GMS depends on the presence of a southern magnetic field as stated earlier [2]. Since the southward field may be contained in the front or back sections of interplanetary CMEs (ICMEs) [20], one expects a large variation in delay time. In more than half of the events (58%), southward component of the interplanetary magnetic field (B_z) immediately follows the shock front making the delay time less.

3.4 *Solar wind*

The arrival of the effects at 1 AU caused by each CME has been determined by careful examination of IMF and solar wind data obtained from ACE Spacecraft. One obvious parameter from the solar wind data is the speed of interplanetary CME (ICME) which can be used to calculate the maximum travel time of CME from the Sun after its occurrence on the solar disk to the near Earth space at the onset of GMS. The calculated time on the basis of solar wind data is the maximum possible travel time for those CMEs that initially have a high speed at the Sun and maintain or decrease the speed in their course towards the Earth [2].

The minimum and maximum values of SW velocity (V_{SW}) when storm is at its peak are 345 km/s and 978 km/s for intense GMSs, with an average speed of 518.5 km/s. Fourty-two per cent events are found to have speed more than the average speed. For superintense GMSs, the minimum and maximum values are 584 km/s and 970 km/s, with an average speed of 748.5 km/s and 50% of the total events have speed above the average speed.

For different values of the solar wind velocity (V_{SW}), the disturbance storm time index (Dst) has been plotted in figure 3. The good correlation between them shows very clearly the dependence of Dst on V_{SW} leading to the view that SW plasma of high speed leads Dst to its minimum value much lesser and hence, making the storm more intense. Thus, V_{SW} seems to be an important parameter in determining the nature of GMSs. Further, the correlation between the maximum value

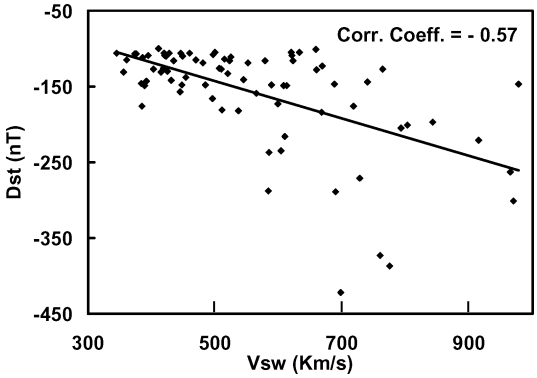

Figure 3. The dependence of minimum value of Dst index when the storm is at its peak with the SW velocity.

of SW velocity during the entire period of GMS and Dst minimum has also been investigated but the dependence is quite poor ($r = -0.43$).

3.5 *Association of GMSs with solar features*

Since the CMEs take 1 to 5 days to reach the Earth [9,11,21], five-day interval prior to the onset of GMSs has been considered. As stated earlier, during solar maxima, an average of 2 to 3 CMEs/day are observed. Therefore, it is quite likely that a given storm may be sometimes associated with more than one CME, which is also quoted by Zhang *et al* [18] and to choose the appropriate CME associated with a particular GMS is not an easy task [10] during that particular event. Out of the total of 67 intense GMSs investigated during the 11-year period, 27% are associated with single CMEs and 63% are associated with multiple CMEs. Further, 63% of the total intense events are associated with full halo CMEs, whereas 27% are associated with partial halo CMEs. Since, the speed and angular width of CMEs increase during its propagation, we cannot ignore that some exceptional cases may be associated with narrow CMEs [2,8]. Therefore, rest of the 10% cases may be associated with narrow CMEs with slowly increasing in its angular width and getting accelerated during its path or it might be due to SF or may be due to corotating interaction regions (CIRs) which is a rare possibility [11]. Somehow, it may not be overlooked.

Ninety-four per cent of the superintense events investigated, are found to be associated with full halo CMEs, while 6% events are found to be associated with partial halo CMEs. Twenty-nine per cent have single CME dependence, whereas 71% have multiple CME association, which are all halo or combination of halo and partial halo. Therefore, the present study reveals that majority of the GMSs with Dst <-100 nT are associated with multiple CMEs which is contradictory to the findings of Zhang *et al* [18]. Somehow, this is in agreement with the findings of Gopalswamy *et al* [11].

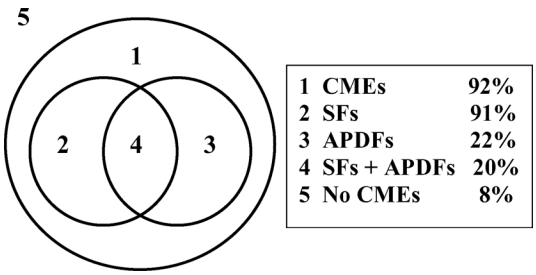

Figure 4. Association of different solar features with intense and superintense (i.e. total) GMSs.

Thus, 92% of the total events both intense and superintense are found to be associated with CMEs, may be single or multiple, halo or partial halo. When these 92% events are further investigated for other solar features, it is found that 91% of them are associated with X-ray SFs as well, whereas, 22% events are associated with APDFs which is shown by the Venn diagram in figure 4. Fifty-six per cent SFs are found to be of major importance, i.e. they belong to M and X classes, which is almost the same as observed by Zhang *et al* [18] for the period 1996–2005. Thus, GMSs of high intensity appear to be mainly associated with CMEs of varying nature followed by SFs of high importance.

3.5.1 *Initial speed of CMEs.* In the present study the linear speed derived from the height–time plot is considered as the initial speed of CME [2,8]. The minimum and maximum speeds of CMEs observed for intense GMSs are 108 km/s and 2861 km/s respectively, whereas for superintense GMSs, the minimum and maximum speeds are 453 km/s and 2459 km/s respectively.

The halo CMEs as a class are much faster on the average. The actual width of halo CMEs is not known but they are generally expected to be much wider than the average CMEs which means that they are more energetic [11]. It is also clear from the present study that except one event of November 5, 2001, all (94%) of the superintense events and 63% of the intense events are high-speed events with speed more than 700 km/s.

The weak dependence ($r = -0.2$) between V_{CME} and the Dst associated with GMSs indicate that the initial speed may not be used as the parameter for predicting geomagnetic activity similar to what is being observed by Zhang *et al* [2] and Cid *et al* [10]. Somehow, the variation in the velocity of CME along with some other parameters, as the CME propagates from the sun towards Earth, may be used to predict the GMS.

3.5.2 *Travel time of CMEs.* Travel time is the time taken by CME initiated at the Sun to arrive at near Earth distance. Different authors have defined this travel time in different ways [2,3,22]. We have taken travel time (TTI) of CME to 1 AU distance as the difference between the time of occurrence/initiation of CME at solar disk and the time at the onset of GMSs. The travel time is an important parameter which helps in assessing the time available for CME to arrive at 1 AU prior to the commencement of GMSs. The travel time depends on the initial speed of the CME [23]. In the present analysis, the minimum travel time is found to be 23.5 h and a

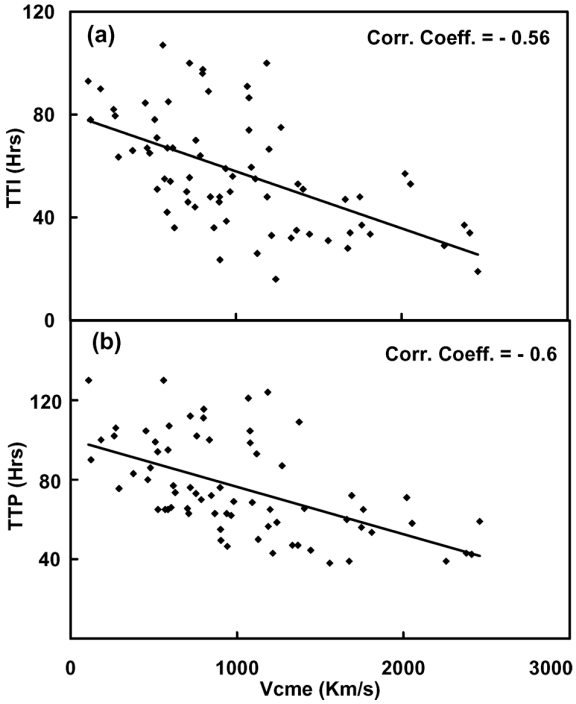

Figure 5. The dependence of arrival time of CME. (**a**) at 1 AU distance (TTI); (**b**) when the storm is at its peak (TTP) on the initial velocity of CME.

maximum of 117.5 h for intense cases, whereas the minimum and maximum travel time for superintense events are 28 h and 91 h respectively. Some exceptional cases for very less travel time of just 16 h is observed on 18 April 2002 for intense GMS and 19 h is observed on 29 October 2003 for superintense GMS. However, the pretty high velocities of 1240 km/s and 2459 km/s of the respective halo CMEs justify its association with the storm. Such types of exceptional cases are also observed by Gopalswamy *et al* [11]. The dependence of the travel time (TTI) of geoeffective CMEs on their initial speeds as measured by LASCO coronagraph is shown in figure 5a.

Further, the travel time of CME from solar disk upto the time when GMS is at its peak (TTP) against initial velocity of CME is shown in figure 5b. Almost similar dependence is observable from figure 5b as it is depicted by TTI. Four contradictory findings are also observed where the TTI or TTP are high along with the high velocity of CME or vice versa. These exceptional cases can be taken care of by the fact that CMEs accelerate or decelerate during their propagation [8,11].

3.5.3 *Distribution of geoeffective CMEs on solar disk.* The locations of CMEs for intense and superintense GMSs have been plotted in figure 6. It is observable from figure 6 that 43% of the geoeffective CMEs appear from the East of the central meridian, whereas 57% appear from the west side. Thus, the distribution is

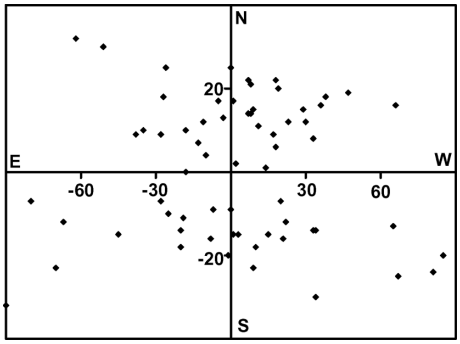

Figure 6. Location of CMEs on solar disk for intense and superintense GMSs during solar cycle-23.

asymmetrical as also observed by Zhang *et al* [2,18], Gopalswamy *et al* [11] and Wang *et al* [22] and is contrary to the observations of Srivastava and Venkatakrishnan [3] and Cane *et al* [9]. Thus, figure 6 shows that the longitude distribution of strongly geoeffective CMEs has a clear western bias. Eighty-two per cent of the total events observed originated within $\pm 45^\circ$ of the central meridian. Therefore, geoeffective halos causing intense and superintense GMS are mainly the disk events, i.e. longitudes confined within $\pm 45^\circ$ and not the limb events where the longitude is confined between 45° and 90° [11].

Further, it is also apparent from figure 6 that there exists hemispherical bias in halo CMEs that reach the Earth, in contrast to the observations of Srivastava and Venkatakrishnan [3]. Fifty-five per cent events are reported in northern hemisphere, whereas 45% events have occurred in southern hemisphere. All the events are observed within $\pm 32^\circ$ of the equator suggesting that geoeffective CMEs are generally confined close to the equator and they occur at low and moderate latitudes as it is apparent from figure 6.

Location of CMEs is also studied for the rising and declining phases separately. Western bias is clearly visible in both the phases, whereas no hemispherical asymmetry is observed in the declining phase. In the rising phase, 63% events have occurred in northern hemisphere which reduces to 50% in declining phase.

3.6 *Storm duration and successive storms*

The duration of the storm is found to be different in different cases. Some storms end up in few hours like that of 23 May 2002 which ended up in just 13 h while some gets prolonged to few days like the one of 07 November 2004 which extended up to 132 h (i.e. 5.5 days). In a peculiar case of intense GMS of 11 February 2004, the storm extended up to 3.5 days with the minimum Dst value of -109 nT. However, it is not found associated with any halo or partial halo CMEs. A flare of very low class, i.e. B4.4 is observed during that time. Another typical case of intense GMS is observed on 29 November 2000, where the storm ended up in less than a day (22 h) while minimum Dst value is found to be -119 nT and six halo and three

partial halo CMEs are observed in 5-day window. Thus, there is no relation between the storm duration and the number of CMEs involved in its occurrence.

Further, in some of the cases like that of 15 July 2000, where Dst index falls to −301 nT, only one CME is observed. On the other hand, nine CMEs are observed to cause the GMS of 29 November 2000 with the Dst value of −119 nT. Hence, the intensity of the GMS also does not reveal any relationship with the number of CMEs involved in its occurrence.

In some of the events, successive storms are observed, i.e. either the next storm started just after the end of the previous storm or the next storm started while the previous one is in progress. Seven storm doublets and four storm triplets are observed during the said period where the GMS follows the criteria of Dst <-100 nT. Contrary to Zhang *et al* [2] and Gopalswamy *et al* [11], where they have treated successive storms as single event, each storm has been analysed as separate entity in the present study since they seem to be associated with different CMEs. Their combined effect makes the GMS complex by having a very high value of solar wind velocity continuously for a long period. In the present study, SW is observed to be complex for 2 to 6 days during collective storms. This might be due to successive evolution of CMEs and their interaction during their propagation through interplanetary space.

3.7 *Influence of IMF on geomagnetosphere*

In order to understand the response of the magnetosphere to IP conditions, IMF strength (B) and its north–south component (B_z) with Dst are plotted in figures 7a and b. In all the intense events, the value of B_z is ≤ -9 nT, whereas the minimum value of B is 10 nT. For the superintense events, these values are pretty high with $B_z \leq -27$ nT and $B \geq 34$ nT. Figures 7a and b show that there is a good anti-correlation between B and Dst such that as B increases, the Dst is observed to decrease, whereas there is a better correlation between B_z and Dst which indicates that the Dst index, which is a measure of the ring current, increases with the increase in the values of IMF component, B_z. Hence, it is derived from here that B and B_z may also be treated as the reliable predictors of GMS's strength. B_z (GSE) and B_z (GSM) are studied in the present analysis and the correlation coefficient of B_z (GSM) with Dst is 0.75, whereas the correlation coefficient of B_z (GSE) with Dst is 0.73. Thus, both the parameters give almost similar results. However, B_z (GSM) shows somewhat better results.

As stated earlier, V_{SW}, B and B_z show significant correlation with Dst index. Since the GMS is the response of the magnetosphere to IP phenomena arising as a consequence of a solar event [10], the coupling between the Sun–Earth parameters seem essential so as to forecast the magnitude of an impending GMS. To understand the physical mechanism of transference of SW energy into the magnetosphere, which is due to the magnetic reconnection between the IMF and the Earth's magnetic field, is the major aim of solar–terrestrial physics. The correlative study between Dst and the product of V_{SW} with IMF parameters are helpful in understanding the SW–magnetosphere interaction. The strength of the southward IMF or more accurately the dawn–dusk component of the electric field, $E = -V \times B$ describes

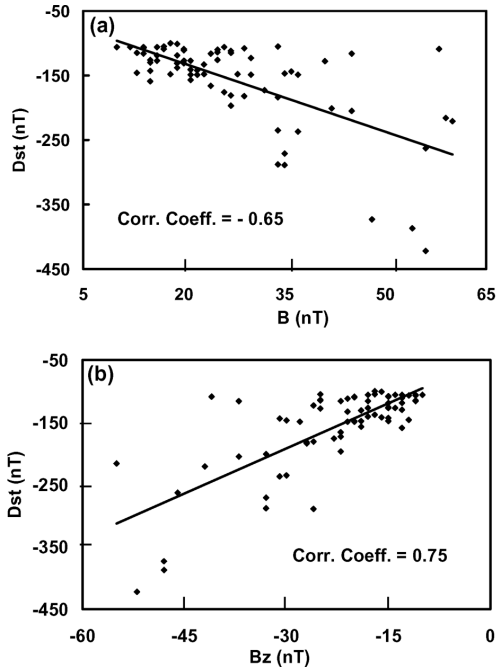

Figure 7. The dependence of Dst index on (**a**) peak value of IMF, B and (**b**) north–south component of IMF, B_z.

this process efficiently [18]. $V_{\rm SW} \cdot B$ and $V_{\rm SW} \cdot B_z$ show a good correlation with Dst index as shown in figures 8a and b. Thus, the geomagnetic activity responds to magnetospheric changes brought about by SW and IMF fluctuations. Correlative studies have clearly demonstrated the usefulness of geomagnetic indices as a tool for understanding the coupling between magnetosphere and IP medium. Hence, $V_{\rm SW} \cdot B_z$ and B_z may be considered as significant contributors in determining the strength of GMSs. Almost similar findings are also made by Srivastava and Venkatakrishnan [3], Singh *et al* [24] and Gopalswamy *et al* [25].

4. Conclusions

Eighty-four GMSs with Dst <-100 nT occurring from January 1996 to April 2006, of solar cycle-23 have been investigated on the basis of their solar sources, IMF/geomagnetic parameters etc. Based on this analysis, the following conclusions have been derived:

1. The number of intense and superintense GMSs show three distinct peaks during the 11-year period of 23rd solar cycle. The largest number of high strength GMSs are observed during maximum phase of solar cycle.
2. There is a minimum time delay of 4 h and a maximum of 56 h between the commencement and the peak time of GMS which is due to the difference in

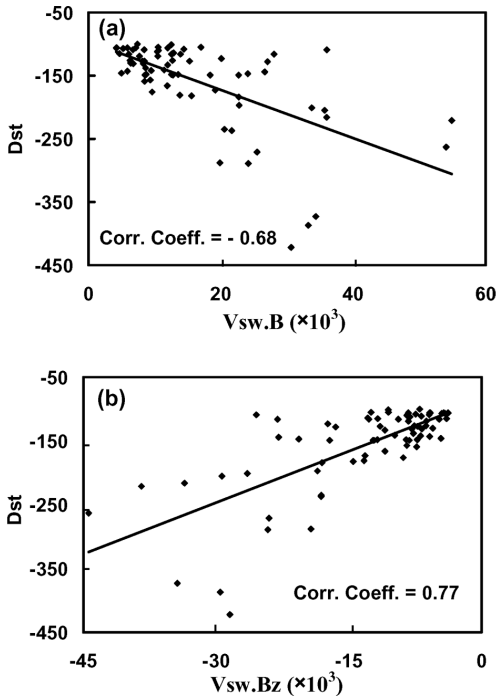

Figure 8. The dependence of Dst index on (**a**) $V_{\rm SW} \cdot B$ and (**b**) $V_{\rm SW} \cdot B_z$.

timings in the striking and reconnection of southward component of IMF with Earth's magnetosphere for different storms. In more than half of the events (58%), B_z immediately follows the shock front.

3. The high speed solar wind plasma may be in the form of CMEs or else is more likely to cause the intense and superintense GMSs. Hence, $V_{\rm SW}$ may be taken as a reliable indicator of strength of GMS.
4. Ninety per cent of the total intense and 100% of the superintense GMSs are found to be associated with full halo or partial halo CMEs. The events are not necessarily associated with single CME. There can be multiple CMEs involved in the occurrence of a GMS.
5. Majority (91%) of the events are associated with X-ray SFs in addition to CMEs, whereas few (22%) events are found to be associated with APDFs as well. Further, more than half of the events are found to be associated with major flares of M and X class.
6. The initial speed of CME at Sun cannot be taken as a parameter in deciding the nature of GMSs. This could be due to the fact that CMEs accelerate or decelerate during their propagation.
7. The time taken by the CME from solar disk to Earth distance when GMS is initiated (TTI) as well as when GMS is at its peak (TTP) bear a good relationship with the initial speed of CME.

8. The geoeffective CMEs show longitudinal as well as hemispherical bias. Most of the events occurred in northern hemisphere and on the west side of the central meridian. The investigation suggests that geoeffective CMEs are generally confined close to the equator and they occur at low and moderate latitudes and are mainly the disk events.
9. No relationship is observed between storm duration and the number of CMEs involved in its occurrence. The intensity of the GMS is also independent of the number of CMEs causing the occurrence of the storm.
10. During successive storms, the GMS becomes complex and acquires high value of solar wind velocity for very long duration than in the case of isolated storm which could be due to successive evolution of CMEs and their interaction during their propagation through interplanetary space.
11. The values of B and B_z are pretty higher for superintense events than for intense events. This indicates that for the occurrence of high intensity GMS, the parameters B and B_z should have high magnitude.
12. The B_z value in GSE and GSM coordinates does not make much difference in the result. However, B_z measured in GSM coordinates shows better relationship with Dst than that measured in GSE coordinates.
13. The parameters B and B_z and products of V_{SW} and IMF parameters contribute significantly in deciding the nature of GMSs. Hence, $V_{\mathrm{SW}} \cdot B_z$ and B_z may be considered as key contributors in determining the strength of GMSs.

Acknowledgements

The authors are highly indebted to various experimental groups for providing data on the Web and extend their warm thanks to Prof. N Gopalswamy and Dr H E Coffey for providing valuable information. The authors are also thankful to the anonymous referee for constructive comments and helpful suggestions.

References

[1] L F Burlaga, K W Behannan and L W Klein, *J. Geophys. Res.* **92**, 5725 (1987)
[2] J Zhang, K P Dere, R A Howard and V Bothmer, *The Astrophys. J.* **582**, 520 (2003)
[3] N Srivastava and P Venkatakrishnan, *J. Geophys. Res.* **109**, A10103 (2004)
[4] N Gopalswamy, *J. Astrophys. Astronomy* **27**, 243 (2006) and references therein
[5] N Gopalswamy, in: *Proc. of the Silver Jubilee Symposium of the Udaipur Solar Observatory*, India, 2002
[6] B T Tsurutani, W D Gonzalez, F Tang, S I Akasofu and E J Smith, *J. Geophys. Res.* **93**, 8519 (1988)
[7] E Echer, M V Alves and W D Gonzalez, *Solar Phys.* **221**, 361 (2004)
[8] P K Manoharan, *Solar Phys.* **235**, 345 (2006)
[9] H V Cane, I G Richardson and O C St Cyr, *Geophys. Res. Lett.* **27**, 3591 (2000)
[10] C Cid, M A Hidalgo, E Saiz, Y Cerrato and J Sequeiros, *Solar Phys.* **223**, 231 (2004)
[11] N Gopalswamy, S Yashiro and S Akiyama, *J. Geophys. Res.* **112**, A06112 (2007) and references therein

[12] http://Solarscience.msfc.nasa.gov/CMEs.shtml/ checked on 10.10.2006
[13] C A Loewe and G W Prolss, *J. Geophys. Res.* **102**, 14209 (1997)
[14] W D Gonzalez, B T Tsurutani and A L C Gonzalez, *Space Sci. Rev.* **88**, 529 (1999)
[15] X P Zhao, *Int. Astronomical Union Symp.*, Russia, No. 223 (2004)
[16] S Kumar and M P Yadav, *Indian J. Radio Sp. Phys.* **31**, 190 (2002)
[17] T Atac and A Ozguc, *Solar Phys.* **233**, 139 (2006)
[18] J Zhang, I G Richardson, D F Webb, N Gopalswamy, E Huttunen, J C Kasper, N V Nitta, W Poomvises, B J Thompson, C C Wu, S Yashiro and A N Zhukov, *J. Geophys. Res.* **112**, A10102 (2007)
[19] C C Wu, R P Lepping and N Gopalswamy, in: *Proc. ISCS Symp. on Solar Variability as an Input to the Earth's Environment* (Slovakia, ESA, 2003) Vol. 1, p. 429
[20] K E J Huttunen, R Schwann, V Bothmer and H E J Koskinen, *Ann. Geophys.* **23**, 625 (2005)
[21] M P Yadav and S Kumar, *Indian J. Radio. Sp. Phys.* **81**, 425 (2007)
[22] Y M Wang, P Z Ye, S Wang, G P Zhou and J X Wang, *J. Geophys. Res.* **107(A11)**, 1340 (2002)
[23] S Kumar and M P Yadav, *Pramana – J. Phys.* **61(1)**, 21 (2003)
[24] Y P Singh, M Singh and Badruddin, *J. Astrophys. Astr.* **27**, 361 (2006)
[25] N Gopalswamy, S Akiyama, S Yashiro, G Michalek and R P Lepping, *J. Atmos. Solar Terr. Phys.* **70**, 245 (2007)